Photoinduced Intramolecular Charge Transfer in 9-Aminoacridinium Derivatives Assisted by Intramolecular H-Bond

Robson Valentim Pereira and Marcelo Henrique Gehlen*

Instituto de Química de São Carlos, Universidade de São Paulo, 13566-590, São Carlos-SP, Brazil

Received: October 26, 2005; In Final Form: March 29, 2006

Fluorochromic dyes derived from 9-aminoacridinium containing a vinylene function with electron withdrawing groups such as diethyl [(acridinium-9-ylamino)methylene]malonate (I), ethyl [(acridinium-9-ylamino)methylene]-cyanoacetate (II), [(acridinium-9-ylamino)methylene]malononitrile (III), are prepared and studied in their monoprotonated form. Absorption spectra of the new dyes are red shifted compared to that of the precursor dye. The observed dual fluorescence and multiexponential decay are ascribed to normal emission from the acridinium chromophore in addition to excited-state intramolecular charge transfer (ESICT) process. However, biexponential decay character is observed only for the dicyano derivative (compound III), whereas for the two other systems, more complex kinetics and a three-component decay is recovered. The analysis of the fluorescence decays in different solvents for the first two compounds reveals two short-lived components in the range of 160−350 ps and 1.1−3.0 ns, related to formation and decay of the ESICT state, plus a third one with decay time of about 9 ns, which is ascribed to the normal emission from the acridinium chromophore as an enol tautomer or as an intramolecular H-bond conformer (closed form tautomer). For the dicyano derivative, in which the absence of carbonyl group precludes the H-bond interaction, the biexponential fitting reveals a slightly fast formation rate of the ESICT state with values on the order of 10^{10} s^{-1}, whereas its decay time is between 0.6 and 3.2 ns, depending on the solvent used.

Introduction

Photoinduced intramolecular charge transfer (ICT) and proton transfer (IPT) processes are two important phenomena well reported in the literature.[1−24] They find great importance and applications in many branches of photochemistry. The ICT process, observed first in 1955 by Lippert,[1,2] is characterized by dual emission related to locally excited (LE) and excited-state intramolecular charge-transfer (ESICT) states. ESIPT, studied initially by Kasha et al.,[16] may have similar dynamics as that of ESICT.[17]

Since the first observation of intramolecular charge transfer in 4-(dimethylamino)benzonitrile (DMABN),[1,2] several other molecular systems have been synthesized to get clues about ESICT mechanism, but many of the molecular systems are DMABN derivatives.[4] The same trends occurred with ESIPT studies, and new compounds with donor and acceptor proton sites, which in some cases may form intramolecular hydrogen bond, have been investigated.[19,20]

Another interesting effect occurs when both phenomena are present in the same molecular systems.[25−37] There are a few studied systems with the mixing of processes: aminosalicylates, benzalidines, 4-(dimethlamino)-1*H*-pyrrolo[2,3-*b*]pyridine (DPP), 2-hydroxy-4-(di-*p*-tolylamino)benzaldehyde, 4-*N*,*N*-dimethyl-amino derivatives, and more recently 2-(2′-hydroxyphenyl)-benzoxazole (HBO) derivatives.

Therefore, due the presence of three excited states (LE, ESICT and ESIPT), a more complex excited-state dynamics emerges, and to establish a mechanism is a difficult task, and in some cases very controversial. For instance, in a recently published work, it has been proposed that the high energy ESIPT state leads to a relaxed ESICT state.[36] On the other hand, formation of ESICT first and through this excited state, a jump to ESIPT state, has been also supposed as a possible mechanism.[37]

In the present contribution, three derivatives of 9-aminoacridinium having strong electron withdrawing groups and ICT dynamics are comparatively studied in terms of their photophysical and photochemical properties. A previous account of the spectroscopy of ethyl [(acridinium-9-ylamino)methylene]-cyanoacetate (II) was recently reported in the literature.[38] In this study, the role of intramolecular H-bond and mixing of the $\pi-\pi^*$ and $n-\pi^*$ on the ESICT process is addressed as new effects in this class of dyes.

Experimental Section

Synthesis of the 9-Aminoacridinium Derivatives. The functionalizations of 9-aminoacridine (9AA) with vinylene groups were obtained from reaction of the free base with diethyl (ethoxymethlene)malonate (giving compound I), ethyl (ethoxym-ethylene)cyanoacetate (compound II), and (ethoxymethylene)-malononitrile (compound III), using similar experimental conditions reported recently in the literature.[38] A 1.2 mmol amount of each vinylene group (Acros Organics, 99%) was added to 1.0 mmol of 9-aminoacridine (free base prepared from 9-aminoacridine hydrochloride (Aldrich Co.) treated with ammonium hydroxide solution and dried at low pressure in desiccator), both dissolved in dry ethanol. The system was gently heated under reflux for 6 h and cooled, and the solvent was evaporated under low pressure. The crude compound was purified through flash chromatography using a concentration gradient of hexane/ethyl acetate. The reaction scheme is shown in Figure 1.

Compound I: Yield: 60%. Yellow solid. Mp: 174 °C.

$C_{21}H_{21}N_2O_4$ (364) Calc: C, 69.23; H, 5.49; N, 7.69. Found: C, 69.20; H, 5.88; N, 7.69.

* Corresponding author. E-mail: marcelog@iqsc.usp.br.

10.1021/jp0561470 CCC: $33.50
Published on Web 05/25/2006

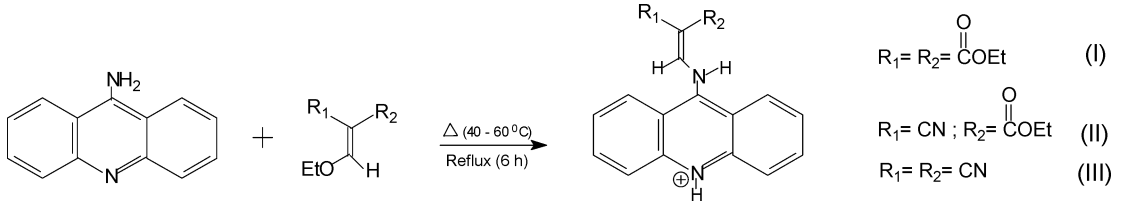

Figure 1. Reaction scheme and molecular picture of the 9AA derivatives.

FTIR (cm^{-1}): 3247 (R_2N-H), 1696 (C═O), 1646 (C═O), 1597 (C═C), 1231 (C−O−C).

^1H NMR ($CDCl_3$): 11.9 (d, $J = 12$ Hz, NH), 8.57 (d, $J = 12$ Hz, ═CH), 8.40 (d, $J = 8.6$ Hz), 8.19 (d, $J = 8.7$ Hz), 7.88 (t, $J = 7.2$ Hz), 7.66 (t, $J = 7.2$ Hz) 8H of acridinium ring, 4.43−4.49 (q, $J = 7.1$ Hz), 4.22−4.28 (q, $J = 7.1$ Hz), 1.45−1.49 (t, $J = 7.1$ Hz), 1.27−1.31 (t, $J = 7.1$ Hz) two OCH_2CH_3. The mass spectrum (LC-MS) resulted in m/z =363.

Compound II: Yield: 35%. Red solid. Mp: 263 °C.

$C_{19}H_{16}N_3O_2$ (318) Calc: C, 69.23; H, 5.49; N, 7.69. Found: C, 69.20; H, 5.88; N, 7.69.

FTIR (cm^{-1}): 3230 (R_2N-H), 2205 (CN), 1666 (C═O), 1631 (C═C), 1233 (C−O−C).

^1H NMR (DMSO): 8.66 (s, ═CH), 8.15 (d, $J = 8.4$ Hz), 7.90 (t, $J = 8.0$ Hz), 7.77 (d, $J = 8.0$ Hz) 7.47 (t, $J = 8.0$ Hz), 8H of acridinium ring, 4.23−4.12 (q, $J = 7.0$ Hz), 1.27−1.20 (t, 7.0 Hz) of OCH_2CH_3. The mass spectrum (LC-MS) resulted in $m/z = 318.2$.

Compound III: Yield: 55%. Orange solid. Mp: 275 °C.

$C_{17}H_{11}N_4$ (271) Calc: C, 72.30; H, 4.10; N, 20.67. Found: C, 73.10; H, 5.03; N, 19.89.

FTIR (cm^{-1}): 3138 (R_2N-H), 2206 (CN) and 2192 (CN), 1633 (C═C).

^1H NMR (DMSO): 8.47 (s, ═CH), 8.26 (d, $J = 7.2$ Hz), 8.03 (t, $J = 7.2$ Hz), 7.89 (d, $J = 8.4$ Hz) 7.61 (t, $J = 8.1$ Hz), 8H of acridinium ring. The mass spectrum (LC-MS) resulted in $m/z = 270$.

Measurements. The FTIR and ^1H NMR spectra were obtained using Bomem MB 102 and Bruker DRX 400 spectrometers, respectively. LC-MC mass spectrum was performed in a Micro mass UK LTD Platform LC, using electron spray interface with a voltage of −25 V (compound I), + 10 V (compound II) and −42 V (compound III). The melting points were measured by using a differential scanning calorimetry (DSC) Shimadzu TA-50 under a nitrogen flow rate of 20 $mL \cdot min^{-1}$. Each sample was heated from 25 to 400 °C at 20 $°C \cdot min^{-1}$ Absorption measurements were performed on a Cary 5G-Varian spectrophotometer, and the corrected steady-state fluorescence spectra were recorded on a Hitachi spectrofluorometer at 298 K. The samples were conditioned in a 1 × 1 cm quartz cuvette, thermostated by circulating fluid through a jacketed cuvette-holder, and in air equilibrated condition. All solvents were distilled and dried in molecular sieves before their use. Fluorescence decays in solution at 298 K were measured by time correlated single-photon counting technique using a CD-900 Edinburgh spectrometer equipped with Glan-Thompson polarizers, and a Peltier cooled PMT (Hamamatsu R955) as photon detector. Fast transients in the picosecond time scale were measured using a homemade spectrometer equipped with Glan-Laser polarizers in magic angle, a Peltier cooled PMT-MCP (Hamamatsu R3809U-50) as photon detector, and Tennelec-Oxford counting electronics. The light pulse was provided by frequency doubling the 200 fs laser pulse of Mira 900 Ti−sapphire laser pumped by a Verdi 5 W Coherent. The laser pulsed frequency was reduced by using a Conoptics pulse picker system. The instrument response functions (irf) of the spectrometers are 700 and 40 ps at fwhm. The fluorescence decays were analyzed by reconvolution procedure with multiexponential decay models. Molecular quantum chemical study was performed using Gaussian 03. The initial molecular geometry were obtained at AM1 semiempirical, and the final geometry optimization were achieved using DFT method with the 6-31G-(d) basis set and B3LYP hybrid exchange-correlation functional.

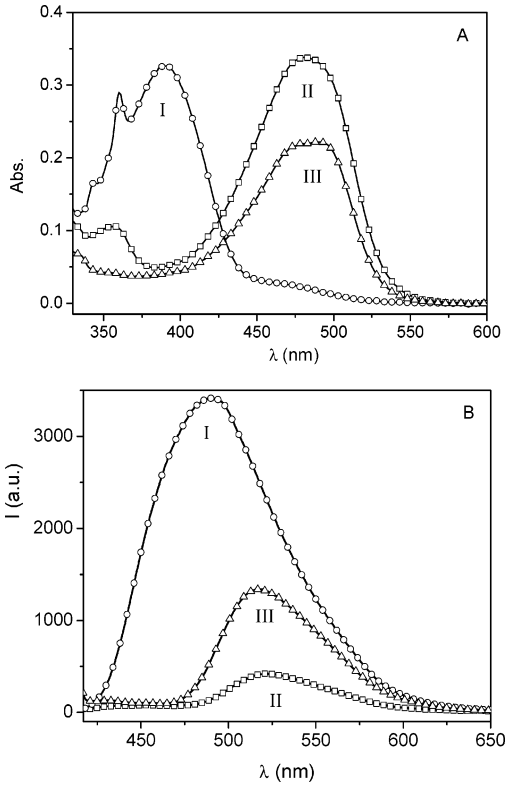

Figure 2. Electronic absorption (A) and emission (excitation at 400 nm) (B) spectra of compound I (○), II (□), and III (△) in 2-propanol at 298 K. The dye concentration was 2×10^{-5} M for all compounds. The extinction coefficient at the absorption near the maximum for I, II and III are ϵ_I(390 nm) = 17 300, ϵ_{II}(482 nm) = 20 300, and ϵ_{III}(492 nm) = 14 600 M^{-1} cm^{-1}.

Results and Discussion

1. Steady-State Measurements. The absorption and emission spectra of compounds I, II, and III were studied in different types of organic solvents. The spectroscopic behavior of these dyes in 2-propanol is shown in Figure 2.

For comparison, the absorption and emission spectra of 9-aminoacridinium (9AA) in 2-propanol is plotted in Figure 3. Contrasting with the precursor 9AA, the derivatives have broad low-energy bands in absorption and in emission as well, which may indicate some degree of optical charge transfer in these derivatives. This CT effect is stronger in II and III that contain the CN electron-withdrawing group.

The electronic spectra of the three compounds are solvent dependent. The absorption, excitation, and emission spectra of

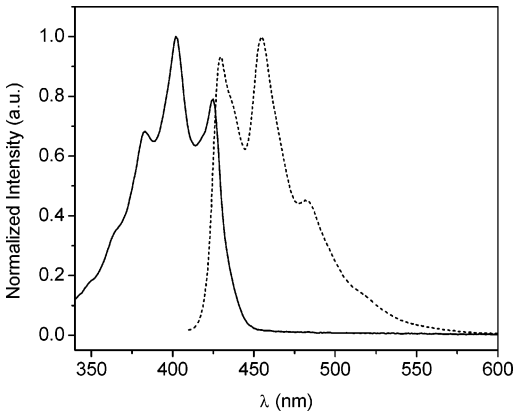

Figure 3. Absorption and emission (excitationa at 400 nm) spectra of 9-aminoacridinium dye in 2-propanol.

I in CCl_4 (polarizable solvent), DMSO (polar aprotic solvent), and in butanol (protic solvent) are given in Figure 4. A significant dependence of the electronic absorption of I with solvent polarity is observed. In CCl_4, the absorption maximum is at $\lambda_{max} = 390$ nm, but the same profile (data not shown) is observed in apolar hexane ($\lambda_{max} = 386$ nm) or in ethyl acetate (385 nm). In polar protic solvent (butanol) two bands are defined, the most intense in the same wavelength region as that observed in CCl_4, in addition to a very weak one shifted to red with maximum at about 460 nm.

In the case of aprotic polar solvent such as DMSO, there are again two bands, but now, the absorption at 460 nm is the more intense (in this solvent, the dye solution of I develops a strong yellow color). Again, the dependence of I with the solvent polarity contrasts with the behavior of its precursor 9AA, which has weak solvent dependent spectral properties. This spectral behavior would indicate some charge-transfer character driven by solvent similar to what was observed with other acridine derivatives reported in the literature.[39]

The emission spectrum of I in those different solvents has a small red shift with an increase of solvent polarity as shown in Figure 4C. Thus, from hexane, ethyl acetate, CCl_4, butanol, and DMSO, the emission maximum is changing from 472, 478, 486, 491, and 499 nm, respectively.

The absorption and emission spectroscopy of II has been already studied recently.[38] Compound II displays a solvent polarity effect that is well explained by Lippert−Mataga solvation model.[40,41] The excited-state dipole moment (μ_e) of II was evaluated as 22 ± 1 D. Following a similar procedure, the excited-state dipole moment of I is estimated to be 14 ± 1 D. The decrease of μ_e of I compared with II is expected because the electron-withdrawing effect of the CN group is predicted to be stronger than that of the COOR group. The absence of emission of III in apolar and in weak polar aprotic solvents has precluded the use of the Lippert−Mataga analysis in an extended range of solvent polarity scale and, therefore, did not allow the evaluation of its μ_e value.

Nevertheless, the absorption and emission spectra of III (see Figure 5) have an interesting behavior in 2-propanol (polar protic solvent), DMSO and *N*,*N*-dimethylacetamide (aprotic polar solvents). The absorption is red shifted in III when compared with I and II. In DMSO, the absorption maximum of III occurs at 434 nm whereas in DMA there is a broad band with maximum at 450 nm and a shoulder at about 500 nm. In 2-propanol, however, the maximum absorption accounts for 494 nm, but a shoulder at 473 nm also appears.

Contrasting with the drastic changes in absorption, the emission is more regular, and III has in these solvents a strong

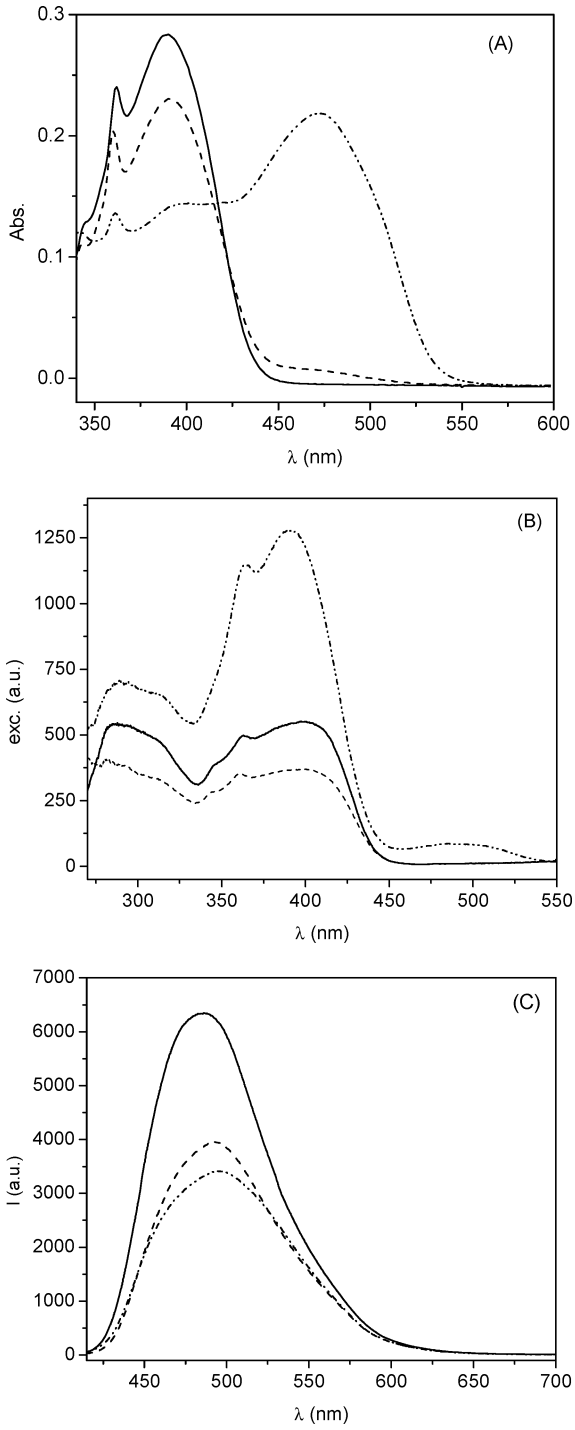

Figure 4. Absorption (A), excitation (B) (emission at 550 nm), and emission (excitation at 400 nm) (C) spectra of I in (—) CCl_4, (---) butanol, and (— ·· —) DMSO.

Gaussian shape band centered at about 522 nm (see Figure 5C). Only in 2-propanol, a weak emission in the region of 425 nm is roughly detected, and it should be ascribed to the emission from acridinium chromophore from a LE state. In a solvent with less specific interaction with the polar groups of compound III like acetonitrile (spectral data not shown), the absorption has a broad band with maximum at 469 nm and the emission maximum occurs at 517 nm, a result that approaches to that observed in 2-propanol but without LE emission. Thus the LE emission of III in alcohols seems to appear as a result of specific solvation of the exocyclic amino group, and this assumption will be confirmed in the spectral study in a mixture of solvents.

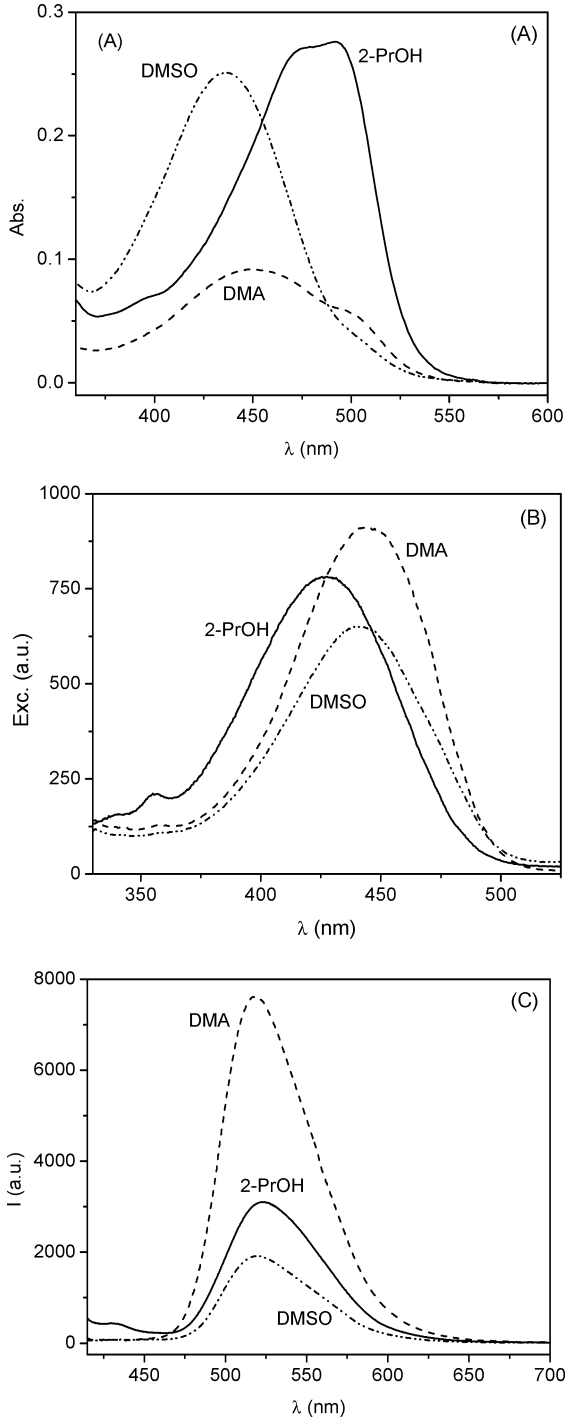

Figure 5. Absorption (A), excitation (B) (emission at 530 nm), and emission (excitation at 400 nm) (C) spectra of III in organic solvents: (—) 2-propanol; (---) DMA; (— ·· —) DMSO.

2. Fluorescence in a Mixture of Solvents. The absorption and emission properties of these 9AA derivatives in solution were shown to be strongly dependent on the type of solvent. In this sense, appropriate solvent mixtures could provide smooth spectral changes with solvent composition. To evaluate the properties of 9AA derivatives in a mixture of solvents, these systems were investigated in 2-propanol by addition of methanol. Figures 6 and 7 are the plot of the absorption and emission of II and III in this solvent mixture, respectively.

The absorption and emission changes of II and III in 2-propanol upon addition of methanol occur in opposite way. For instance, the absorption of II is red shifted upon addition of methanol, and its emission at 520 nm decreases drastically

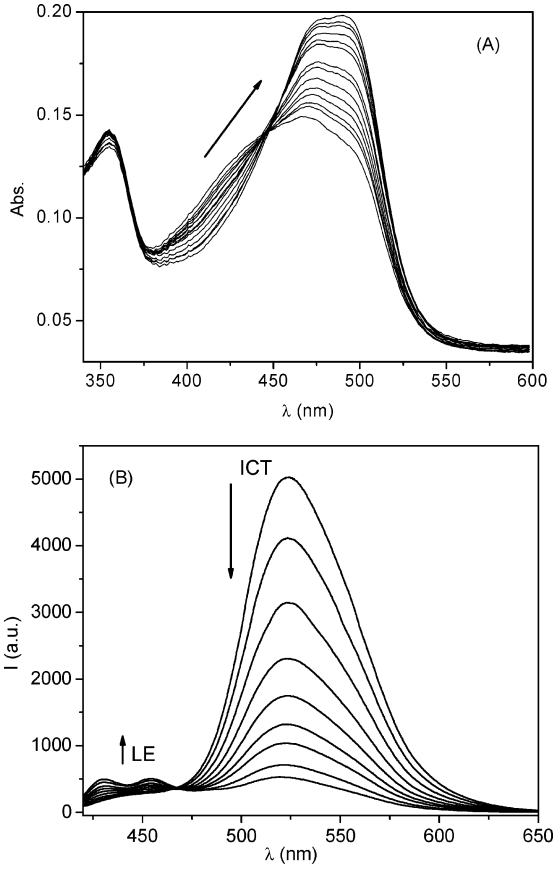

Figure 6. Absorption (A) and emission (B, excitation at 400 nm) spectra of compound II in 2-propanol upon addition of methanol (indicated by the arrow) from 0 to 8 vol %.

with no change in its maximum wavelength. On the other hand, III has absorption blue shift with addition of methanol whereas its emission stays at the same region but with significant increase in its intensity for the first additions (but after addition of more than 20% methanol, the emission of III starts to decrease).

Isosbestic points are observed in both systems, and surprisingly are at the same value of 445 nm. However, only II has an isoemissive point occurring at about 466 nm. In this case, the weak but structured blue emission is the LE emission from acridinium chromophore because its vibronic peaks at about 430 and 455 nm match the maxima observed for 9AA in the same solvent. This spectral trend of II in propanol upon methanol addition is the same behavior found when water is added instead of methanol,[38] and it is not related to protonation-deprotonation equilibrium of the dyes, but it is due to specific solute−solvent interactions (see discussion below). The absorption spectrum of I in 2-propanol does not change appreciable with methanol addition whereas its emission intensity decreases (spectral data not shown), but much less than the changes observed for II.

The quenching effect of the red emission when at least one of the R substituents is a COOEt (emission maxima at $\lambda = 490$ nm and at 520 nm for I and II, respectively) nm in 2-propanol/methanol solvent mixtures can be explained considering the influence of a lone pair of electrons of the 9-amino group.[42] When methanol is added to the system, solvent H-bond with N may occur efficiently, opening a fluorescence deactivation pathway. It changes the amino conjugation effect, keeping the lone pair in resonance only with acridinium ring, but inhibits the extended charge conjugation through the double bound to the cyano and carbonyl electron-withdrawing groups. As a result, there is an increase in the LE structurated emission in the blue

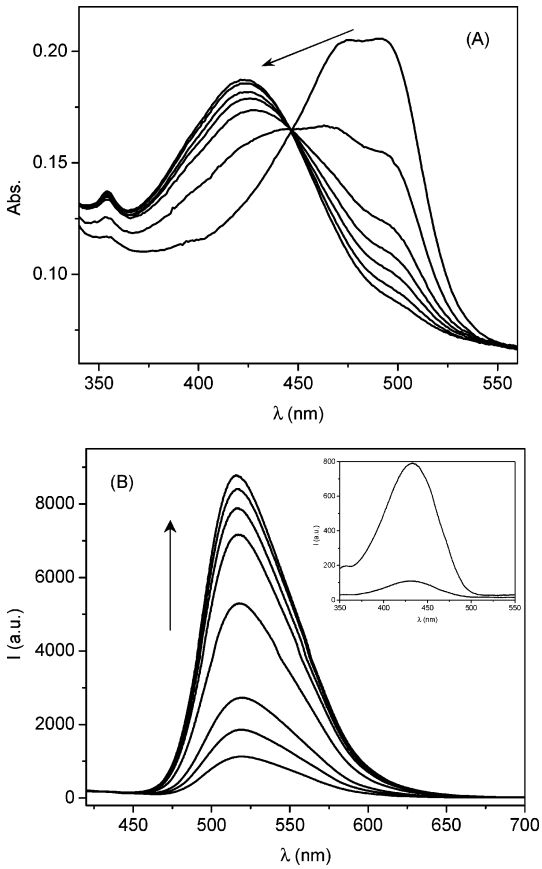

Figure 7. Absorption (A) and emission (B, excitation at 400 nm) spectra of compound III in 2-propanol upon addition of methanol (indicated by the arrow) from 0 to 8 vol %. Inset: excitation spectrum at 0 and 8 vol % of methanol.

TABLE 1: IR Frequencies and Dipole Moments of the 9AA Derivatives[a]

compound	$\bar{\nu}$(CN), cm^{-1}	$\bar{\nu}$(C═O), cm^{-1}	$\bar{\nu}$(N−H), cm^{-1}	μ_g, D[b]	μ_e, D[c]
I		1646 (1713)	3247	8.8	14 ± 1
II	2205 (2228)	1666 (1713)	3230	10.5	22 ± 1
III	2206/2192[d] (2230)		3138	11.5	*e*

[a] Values in parentheses are from the ethoxylate reactant. [b] Ground-state dipole moment of compounds in gas-phase calculated from quantum chemical calculation using DFT (B3LYP) 6-31G(d). [c] Lippert−Mataga analysis. [d] Second $\bar{\nu}$(CN). [e] Absence of emission in solvent of low polarity.

region ascribed to the emission from the acridinium chromophore. The red shift of the absorption spectra of compound II in 2-propanol upon addition of methanol or water (see data discussed in ref 38), is ascribed to a destabilization of a possible intramolecular H-bond conformer (ground-state shifts to high energy level which therefore decrease the energy gap of the electronic absorption causing a redshif of the absorption spectrum). The stabilization of the conformer in a closed form in weak polar solvent may be enhanced by resonance-assisted hydrogen bonding (RAHB) effect.[43−47] Gilli and co-workers have observed RAHB effect in compounds with the β-enaminone moiety. [46] This effect could ultimately lead to a fraction of enol tautomer in less polar solvent (formally a keto-amine/enol-imine equilibrium). The decrease of the IR frequency of the carbonyl and cyano groups is pointed out ground-state charge shift and possible RAHB in I and II (see values in Table 1). It is well know that two descriptors of RAHB are the increase of the ^{1}H NMR δ_{NH} signal and the decrease of the IR frequency

TABLE 2: Fluorescence Decay Components of Acridinium Derivatives in Different Solvents[a]

compound	solvent	τ_1 (ns)	b_1	τ_2 (ps)	b_2	τ_3 (ns)	b_3	χ^2
I	CCl_4	8.2	0.01	159	−0.05	2.95	0.05	1.022
	ethanol	10.4	0.01	149	−0.10	2.27	0.09	1.068
	1M2P	7.3	0.02	151	−0.04	1.77	0.04	1.071
	DMSO	8.8	0.03	171	−0.15	1.34	0.08	1.049
II	CCl_4	8.3	0.01	160	−0.53	2.95	0.48	1.022
	ethanol	9.0	0.02	350	−0.24	1.14	0.08	1.076
	1M2P	7.7	0.01	190	−0.54	3.23	0.48	1.087
	DMSO	8.7	0.02	210	−0.84	1.43	0.71	1.092
III	ethanol			120	−0.01	0.59	0.17	1.085
	1M2P			106	−0.01	3.19	0.05	1.065
	DMSO			148	−0.05	1.67	0.06	1.088

[a] Excitation wavelength at 400 nm, emission wavelength at 520 nm, $T = 298$ K. Results from global analysis of 3 or 4 decays.

of the ν_{NH} when compared with nonresonant similar compounds. For I and II, the values of the δ_{NH} signal are 11.9 and 12.3 ppm, respectively. The ν_{NH} frequencies are listed in Table 1. For weak H-bond, δ_{NH} is between 7 and 9 ppm, and for the free N−H, $\nu_{NH} = 3400$ cm^{-1}, whereas for strong H-bond, δ_{NH} is about 15 ppm and $\nu_{NH} \leq 3000$ cm^{-1}. Thus, any RAHB effect present in I and II is only moderate, and such behavior could be explained by the presence of the OC_2H_5 substituent, which is somewhat decreasing the oxygen proton affinity and, therefore, is weakening the RAHB effect. The intramolecular H-bond and the formation of a close form conformer are predicted from the optimized geometry of I and II. The O···H distance is 1.771 and 1.778 Å for I and II, respectively, which make these interactions as moderate hydrogen bonds.[47] Moreover, the values found in simulation are within the range of experimental data for a series of β-enaminones with values of H-bond distances between 1.65 and 1.83 Å as determined by Gilli.[46]

Nevertheless, a closed form conformer (vide infra) of compound I and II should be also an active species in solution (specially in apolar solvents), and it should play an important role in their photophysics of II. In fact, IR frequency signal ν_{NH} of I in CCl_4 solution is found at 3234 cm^{-1}, which is compatible with a moderate RAHB effect.

In the case of the compound III, which does not contain the carbonyl group and, therefore, is unable to form intramolecular H-bond conformer, the solvent effect on the absorption and emission character indicates some weak specific solute−solvent interactions. The increase in emission intensity with solvent polarity by addition of methanol to 2-propanol solution points out that the ICT state is more stable and emissive in polar solvents, as usual. However, specific interaction of the added methanol with the N−H and CN groups is an important issue in the spectroscopic properties of III, similar to what has been described to compound I and II. This specific solvation of the exocyclic NH group stabilizes the ground state and produces a blue shift in absorption.

3. Fluorescence Decays. Time-resolved emission studies in nonpolar and polar (protic and aprotic) solvents were performed to add more information about the excited-state dynamics in these systems. For I and II, the emission decays are well fitted by three-exponential function. For III, biexponential decay function describes the dynamics. The multiexponential decay behavior occurs for all systems studied but only when they are excited in the UV region (400 nm). The measured decay times and their respective amplitudes (preexponential factors) for these 9AA derivatives in different solvents with excitation in 400 nm are listed in Table 2.

The triexponential decay behavior observed for I and II, in both polar and nonpolar solvents, indicates a three-state dynam-

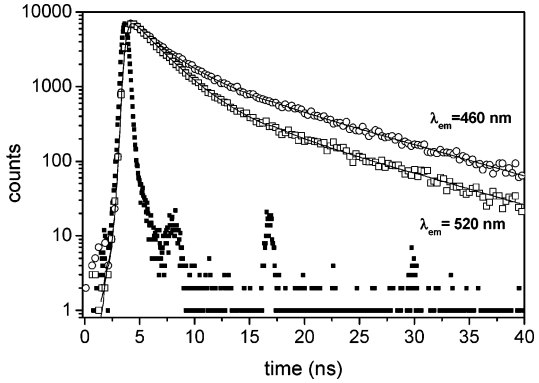

Figure 8. Fluorescence decay of compound I in ethanol in two different emission wavelengths: (■) irf, (○) 460 nm, (□) 520 nm, (—) fitting. $\lambda_{exc} = 400$ nm, $T = 298$ K.

ics, which may arise from the interplay between LE and ESICT states and the presence of a tautomer (which could be a closed form H-bond conformer or even an fraction of enol). Although the decay time components reported in Table 1 are the eigenvalues of a three-excited-state system or two-excited-state system, the values found may be associated with major contribution of some of the related species. For instance, the long-lived component τ_1 is of the same order of the lifetime of the precursor dye as previously reported in the literature[48] and, therefore, should account to the fraction of LE state which does not undergo further ICT process. This component has been previously ascribed to the presence of the enol tautomer in a small percent in II.[38] The short decay time τ_2 may be assigned largely to rate formation of ESICT because its amplitude is negative, and τ_3 may be related to the ICT excited-state lifetime. Another interesting characteristic of the derivatives (I and II only) is the change of the relative weight of the long-lived component τ_1 with the emission wavelength. This behavior in the case of I is shown in Figure 8.

In the blue region ($\lambda_{em} = 460$ nm), there is a larger contribution of the long-lived component τ_1, whereas the inverse occurs in the red region ($\lambda_{em} = 520$ nm) where the emission from ICT state becomes more important. Nevertheless, the decay curves at long time have the same slope, indicating that τ_1 is practically wavelength independent (see Figure 8). The absence of carbonyl group in III precludes formation of intramolecular H-bond and, therefore, does not allow the closed form conformer or the enol tautomer to exist. Thus III is a classical dual excited-state system, which explains its biexponential decay observed (see values of τ_2 and τ_3 listed in Table 2). A comparison of the decay behavior of II with III is illustrated in Figure 9. The long-lived component well detected in II is absent in III. However, for the three compounds, the rates of ICT formation ($1/\tau_2$) from the prompt excitation to the LE state using $\lambda_{exc} < 400$ nm are similar, and the same trend occurs with the decay rate of the ICT excited state (see values of τ_2 and τ_3 listed in Table 2).

In the previous work,[38] an energy diagram of ground and excited electronic states and possible interconversion pathways was discussed for compound II. This diagram is given in Figure 10.

From the analysis of the energy diagram, it is predicted that direct excitation to the ICT state (i.e., an optical transition in the red part of the absorption spectrum) should result in a single-exponential decay for the three compounds if no conversion to upper states occurs. The observed decay of the three systems upon excitation of the ICT absorption band at $\lambda_{exc} = 440$ nm in 1-methyl-2-pyrrolidone (1M2P) are given in Figure 11. In fact, the prediction is confirmed: single exponential behavior

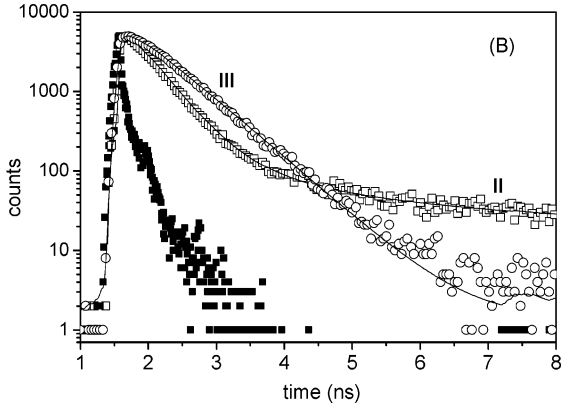

Figure 9. Fluorescence decay of compound II and III in ethanol: (■) irf, (□) compound II, (○) compound III, and (—) fitting. $\lambda_{exc} = 400$ nm, $T = 298$ K.

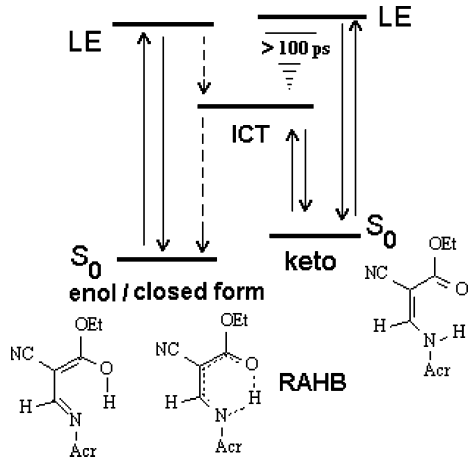

Figure 10. Electronic energy diagram and main excited-state processes. Acri = acridinium moiety. All energy levels are solvent dependent. The tautomeric interconversion between enol/closed forms with keto species is not shown.

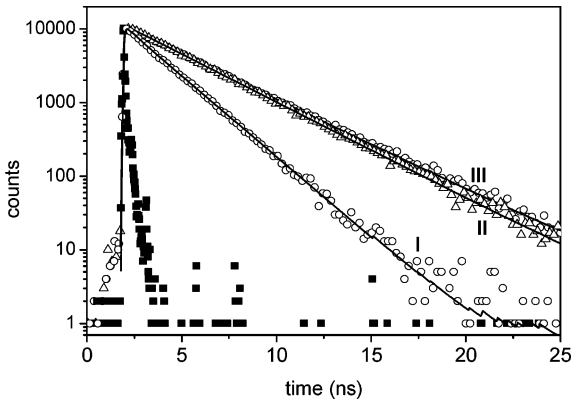

Figure 11. Decay traces of compound I (○), II (△), and III (□) in 1-methyl-2-pyrrolidone at 298 K obtained by excitation at 440 nm of the ICT absorption band. (■) irf.

is observed for all three compounds, and the lifetimes measured, 1.97 ns for I, 3.52 ns for II and 3.32 ns for III, are practically equal to the values of τ_3 listed in Table 2.

However, an open question is why the rate of conversion of upper excited LE state into ICT state is slow ($\tau_2 > 100$ ps), because the presence of the LE and optical charge-transfer absorption bands would indicate a possible strong coupling of S_0 and ICT states. One explanation is that LE and ICT absorptions are of $\pi-\pi^*$ character, but the transition moment of the upper LE is parallel to the short axis of the acridinium

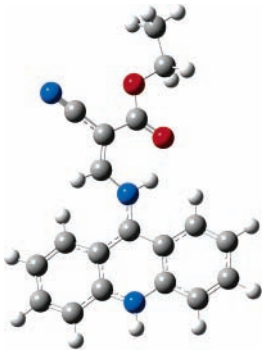

Figure 12. Molecular structure of compound II obtained by DFT/B3LYP 6-31G(d) optimization method. The dihedral angle between the acridinium π system and the 9-aminomethylene group is 32°, and the N−H···O distance is 1.778 Å.

ring (La transition), whereas the ICT has its transition moment toward the electron-withdrawing $R_{1,2}$ groups through the vinylene bond. Thus the ICT formation from the LE upper state should involve a molecular torsion, following a kind of twisted intramolecular charge-transfer mechanism (TICT) involving the exocyclic NH group. In fact, from calculated geometry, the dihedral angle between the acridinium π system and the 9-aminomethylene group is 29.20, 32.25, and 34.74°, for compounds I, II, and III, respectively. On the other hand, the mixing of the of $\pi-\pi^*$ and $n-\pi^*$ states due to the presence of NH group intercalating the acridinium and $R_{1,2}$ should define the ICT state as a manifold of close states, and no pure $\pi-\pi^*$ character is present, which should reduce the transition probability of LE to ICT by orbital symmetry condition. A molecular structure of II obtained by quantum chemical calculation is given in Figure 12.

The calculations indicate that the ground state has a large contribution of an imine form of the exocyclic nitrogen (=N−H) due to the presence of the electron-withdrawing groups. The tautomerism of the 9AA and of its derivatives is well stablished in the literature.[49,50] Following this argument, the strong red absorption band in polar solvents would originate from a π-conjugated extended effect because the 9AA moiety has contribution of an imine form. Note that in such tautomeric imine form, the endocyclic N of the acridine ring becames the center of an electron donor group, and the resonance favors a charge-transfer toward the electron withdrawing groups through the vinylene molecular bridge (see Figure 13 below).

However, when the RAHB effect is operative, there is a necessary blocking of the amine−imine resonance of the acridinium ring, because the exocyclic N is pushing to an enol−imine form that do not allow such resonance anymore (see the enol/closed form in Figure 10). This is clear from the analysis of the absorption spectra of Figure 4A where compound I in apolar solvent (where the enol is present) has a strong band at about 400 nm, but in polar solvent (where the keto form is present and therefore the amine-imine tautomerism of the acridinium takes place) there is a strong red band at about 470 nm ascribed to a π-conjugated extended effect and charge transfer. A similar CT optical transition was observed in the study of push−pull polyenes with donor and acceptor end groups. [51]

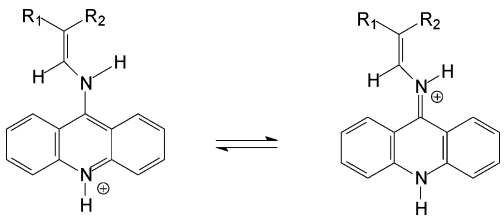

Figure 13. Amine−imine tautomerism of the 9AA derivatives.

Conclusions

The 9AA derivatives with strong electron withdrawing groups have a very complex excited-state kinetics characterized by emission of acridinium chromophore in its locally excited (LE) singlet states in addition to red emission from species formed by excited-state intramolecular charge transfer (ESICT). The presence of carbonyl group in compounds I and II makes large differences when compared with compound III, which contains two CN groups. This result is ascribed to an intramolecular H-bond interaction modulated by solvent, and such interaction can give rise to tautomeric species such as a closed-form H-bond conformer or even a small fraction of an enol tautomer.

Acknowledgment. This work was supported by FAPESP and CNPq Brazilian research funds. R.V.P. thank CNPq for graduate fellowship.

References and Notes

(1) Lippert, E.; Lüder, W.; Moll, F.; Nägele, W.; Boos, H.; Prigge, H.; Seibold-Blankenstein, I. *Angew. Chem.* **1961**, *73*, 695.
(2) Lippert, E.; Lüder, W.; Boos, H. *Advances in Molecular Spectroscopy*; Mangini A., Ed.; Pergamon Press: Oxford, U.K., 1962; pp 433 ff.
(3) Grabowski, Z. R.; Rotkiewicz, K.; Siemiarczuk, A.; Cowley, D. J.; Baumann, W. *Nouv. J. Chim.* **1979**, *3*, 443.
(4) Grabowski, Z. R.; Rotkiewicz, K.; Rettig, W. *Chem. Rev.* **2003**, *103*, 3899.
(5) Schuddeboom, W.; Jonker, S. A.; Warman, J. M.; Leinhos, U.; Kühnle, W.; Zachariasse, K. A. *J. Phys. Chem.* **1992**, *96*, 10809.
(6) Zachariasse, K. A.; Druzhinin, S. I.; Bosch, W.; Machinek, R. *J. Am. Chem. Soc.* **2004**, *126*, 1705.
(7) Van der Auweraer, M.; Grabowski, Z. R.; Rettig, W. *J. Phys. Chem.* **1991**, *95*, 2083.
(8) Techert, S.; Zachariasse, K. A. *J. Am. Chem. Soc.* **2004**, *126*, 5593.
(9) Ma, L. H.; Chen, Z. B.; Jiang, Y. B. *Chem. Phys. Lett.* **2003**, *372*, 104.
(10) Sumalekshmy, S.; Gopidas, K. R. *J. Phys. Chem. B.* **2004**, *108*, 3705.
(11) Zhu, A.; Wang, B.; White, J. O.; Drickamer, H. G. *J. Phys. Chem. A* **2003**, *107*, 6932.
(12) Yoshihara, T.; Druzhinin, S. I.; Zachariasse, K. A. *J. Am. Chem. Soc.* **2004**, *126*, 8535.
(13) Silva, A. P.; Gunaratne, H. Q. N.; Gunnlaugsson, T.; Huxley, A J. M.; McCoy, C. P.; Rademacher, J. D.; Rice, T. E. *Chem. Rev.* **1997**, *97*, 1515.
(14) Hermant, R. M.; Bakker, N. A. C.; Scherer, T.; Krijnen, B.; Verhoeven, J. W. *J. Am. Chem. Soc.* **1990**, *112*, 1214.
(15) Goes, M.; Verhoeven, J. W.; Hofstraat, H.; Brunner, K. *ChemPhysChem* **2003**, *4*, 349.
(16) Sengupta, P. K.; Kasha, M. *Chem. Phys. Lett.* **1979**, *68*, 382.
(17) Barbara, P. F.; Walker, G. C.; Smith, T. P. *Science* **1992**, *256*, 975.
(18) Strandjord, A. J. G.; Barbara, P. F. *J. Phys. Chem.* **1985**, *89*, 2355.
(19) Smith, T. P.; Zaklika, K. A.; Thakur, K.; Barbara, P. F. *J. Am. Chem. Soc.* **1991**, *113*, 4035.
(20) Smith, T. P.; Zaklika, K. A.; Thakur, K.; Walker, G. C.; Tominaga, K.; Barbara, P. F. *J. Phys. Chem.* **1991**, *95*, 10465.
(21) Falkovskaia, E.; Sengupta, P. K.; Kasha, M. *Chem. Phys. Lett.* **1998**, *297*, 109.
(22) Bondar, O. P.; Pivovarenko, V. G.; Rowe, E. S. *Biochim. Biophys. Acta* **1998**, *1369*, 119.
(23) Gormin, D.; Sytnik, A.; Kasha, M. *J. Phys. Chem. A* **1997**, *101*, 672.
(24) Guharay, J.; Dennison, S. M.; Sengupta, P. K. *Spectrochim. Acta Part A* **1999**, *55*, 1091.
(25) Heldt, J.; Gormin, D.; Kasha, M. *Chem. Phys.* **1989**, *136*, 321.
(26) Chou, P. T.; Martinez, M. L.; Clements, J. H. *J. Phys. Chem.* **1993**, *97*, 2618.
(27) Chou, P. T.; Martinez, M. L.; Clements, J. H. *Chem. Phys. Lett.* **1993**, *204*, 395.
(28) Ormson, S. M.; Brown, R. G.; Vollmer, F.; Retting, W. *J. Photochem. Photobiol. A: Chem.* **1994**, *81*, 65.
(29) Sytnik, A.; Gormin, D.; Kasha, M. *Proc. Natl. Acad. Sci. U.S.A.* **1994**, *91*, 11968.

(30) Dennison, S. M.; Guharay, J.; Sengupta, P. K. *Spectrochim. Acta Part A* **1999**, *55*, 1127.
(31) Kim, Y.; Yoon, M.; Kim, D. *J. Photochem. Photobiol. A: Chem.* **2001**, *138*, 167.
(32) Chou, P. T.; Liu, Y.; Liu, H.; Yu, W. *J. Am. Chem. Soc.* **2001**, *123*, 12119.
(33) Zhu, A.; Wang, B.; White, J. O.; Drickamer, H. G. *J. Phys. Chem. B* **2004**, *108*, 891.
(34) Chou P. T.; Yu, W.-S.; Cheng, Y.-M.; Pu, S.-C.; Yu, Y.-C.; Lin, Y.-C.; Huang, C.-H.; Chen, C.-T. *J. Phys. Chem. A* **2004**, *108*, 6487.
(35) Chou, P. T.; Huang, C.-H.; Pu, S.-C.; Cheng, Y.-M.; Liu, Y.-H.; Wang, Y.; Chen, C.-T. *J. Phys. Chem. A* **2004**, *108*, 6452.
(36) Seo, J.; Kim, S.; Park, S. Y. *J. Am. Chem. Soc.* **2004**, *126*, 11154.
(37) Douhal, A.; Sanz, M.; Carranza, M. A.; Organero, J. A.; Santos, L. *Chem. Phys. Lett.* **2004**, *394*, 54.
(38) Pereira, R. V.; Ferreira, A. P. G.; Gehlen, M. H. *J. Phys. Chem. A* **2005**, *109*, 5978.
(39) Herbich, J.; Kapturkiewicz, A. *J. Am. Chem. Soc.* **1998**, *120*, 1014.
(40) Lippert, E. Z. *Z. Elecktrochem.* **1957**, *61*, 962.
(41) Mataga, N.; Kaifu, Y.; Koizumi, M. *Bull. Chem. Chem. Soc. Jpn.* **1956**, *29*, 465.
(42) Yang, J. S.; Chiou, S. Y.; Liau, K. L. *J. Am. Chem. Soc.* **2002**, *124*, 2518.
(43) Gilli, G.; Bellucci, F.; Ferretti, V.; Bertolasi, V. *J. Am. Chem. Soc.* **1989**, *111*, 1023.
(44) Bertolasi, V.; Gilli, P.; Ferretti, V.; Gilli, G. *Acta Crystallogr. B51*, **1995**, 1004.
(45) Bertolasi, V.; Gilli, P.; Ferretti, V.; Gilli, G.; Vaughan, K. *New J. Chem.* **1999**, *23*, 1261.
(46) Gilli, P.; Bertolasi, V.; Ferretti, V.; Gilli, G. *J. Am. Chem. Soc.* **2000**, 122, 10405.
(47) Steiner, T. *Angew. Chem., Int. Ed.* **2002**, *41*, 48.
(48) Oliveira, H. P. M.; Camargo, A. J., de Macedo, L. g. M.; Gehlen, M. H.; da Silva, A. B. F. *J. Mol. Struct.* **2004**, *674*, 213.
(49) Rak, J.; Skurski, P.; Gutowski, M.; Jóźwiak, L.; Błażejowski, J. *J. Phys. Chem. A* **1997**, *101*, 283.
(50) Wróblewska, A.; Meszko, J.; Krzymiński, K. Ebead, Y. Błażejowski, J. *J. Chem. Phys.* **2004**, 303, 301.
(51) Slama-Schwok, A.; Blanchard-Desce, M.; Lehn, J. M. *J. Phys. Chem.* **1990**, *94*, 3894.